

Siamese Anchor Proposal Network for High-Speed Aerial Tracking

Changhong Fu^{1,*}, Ziang Cao², Yiming Li³, Junjie Ye¹, and Chen Feng³

Abstract—In the domain of visual tracking, most deep learning-based trackers highlight the accuracy but casting aside efficiency, thereby impeding their real-world deployment on mobile platforms like the unmanned aerial vehicle (UAV). In this work, a novel two-stage siamese network-based method is proposed for aerial tracking, *i.e.*, stage-1 for high-quality anchor proposal generation, stage-2 for refining the anchor proposal. Different from anchor-based methods with numerous pre-defined fixed-sized anchors, our no-prior method can 1) make tracker robust and general to different objects with various sizes, especially to small, occluded, and fast-moving objects, under complex scenarios in light of the adaptive anchor generation, 2) make calculation feasible due to the substantial decrease of anchor numbers. In addition, compared to anchor-free methods, our framework has better performance owing to refinement at stage-2. Comprehensive experiments on three benchmarks have proven the state-of-the-art performance of our approach, with a speed of ~ 200 frames/s.

I. INTRODUCTION

In recent years, aerial tracking has received considerable attention because of its wide applications such as indoor obstacle avoidance [1], disaster response [2], and mounting sensors [3]. The objective of aerial tracking is to predict the location of the object in the following frames based on its initial state. One remarkable difference between aerial tracking and general tracking is that aerial tracking requires real-time speed and low energy consumption due to the resource-constrained aerial platforms. Besides, aerial tracking suffers from various challenging scenarios introduced by unmanned aerial vehicle (UAV), *e.g.*, fast motion, low resolution, and severe occlusion. Based on the aforementioned property of aerial tracking, one question is raised naturally: *can we find a good balance between efficiency and robustness, and develop an efficient and effective aerial tracker?*

In literature, aerial tracking approaches are mainly divided into two types: correlation filter-based online trackers which are CPU friendly [4]–[6], and deep learning-based offline trained trackers that need a high-end GPU [7], [8]. Though the former is low-cost and energy-efficient, the performance still has a clear gap compared to the latter taking advantage of the offline training. However, the latter is suffering from low efficiency. To achieve a satisfactory balance between performance and speed, this work tries to improve deep trackers’ performance while lowering their redundancy.

*Corresponding Author

¹Changhong Fu, Ziang Cao, and Junjie Ye are with the School of Mechanical Engineering, Tongji University, 201804 Shanghai, China. changhongfu@tongji.edu.cn

²Ziang Cao is with the School of Automotive Studies, Tongji University, 201804 Shanghai, China.

³Yiming Li and Chen Feng are with the Tandon School of Engineering, New York University, NY 11201 New York, United States.

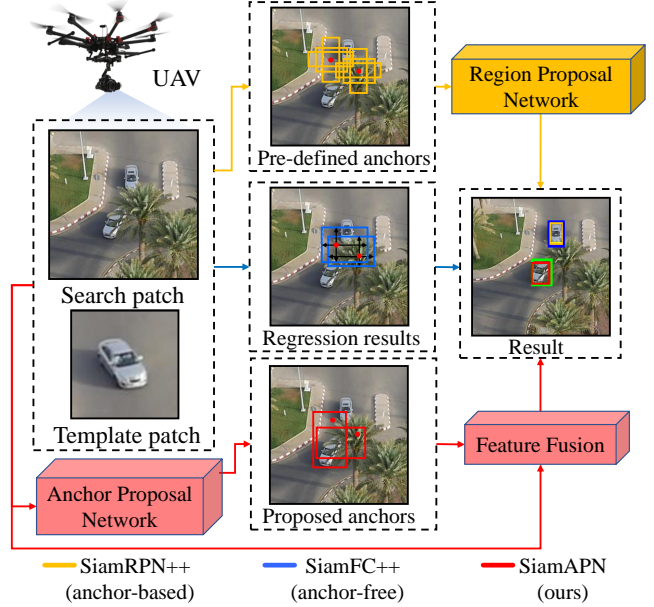


Fig. 1. Comparison with the other two cutting-edge methods, *i.e.*, anchors-based method (SiamRPN++ [9]) and anchor-free method (SiamFC++ [10]) on *car7* from UAV123@10fps [11]. The green box represents the ground truth bounding box. The adaptive anchors generated by APN can improve the perception of SiamAPN, making our tracker straightforward to notice the occluded car. Meanwhile, the APN merely generates one no-prior anchor at each point on feature map, reducing a large number of anchors and hyper-parameters significantly.

Among the deep learning-based trackers, the siamese-based trackers play important roles in object tracking [9], [10], [12]–[14]. The anchor-based method was put forward firstly in SiamRPN [12]. Then, SiamRPN++ [9] achieves state-of-the-art performance with more elaborate architecture. Since traditional anchors are introduced for region proposal, RPN-based trackers are sensitive to the numbers, sizes, and aspect ratios of anchor boxes. Moreover, the hyper-parameter tuning is quite essential to obtain successful tracking results. To deal with the problems, the anchor-free method was proposed which directly predicts the four offsets compared to the object center [10]. Different from [10], our method reduces hyper-parameters hugely while utilizing the advantages of anchors by redesigning the anchor generation module.

Instead of using several pre-defined anchors at each location, this work uses an anchor proposal network (APN) to generate one high-quality anchor at each point on feature map by regressing four offsets, thereby reducing the computation and boosting the tracking efficiency. The APN also balances the negative and positive samples during offline training, increasing the utilization of anchors. Furthermore,

the APN makes the proposed anchors more adaptive and sensitive than pre-defined unchanged anchors, thereby improving the robustness against fast-moving and occluded objects with small scales. The comparison of anchor-based [9], anchor-free [10], and our method is shown in Fig. 1. When the object is fully or partially occluded, the feature of objects highly decreases and similar objects will become more obvious on the feature map, which could induce the trackers to make false judgments. In virtue of the adaptive anchor proposal generation, our method can find out the areas where the object is most likely to exist, making light work of the classification. Besides, SiamAPN maintains the robustness of the proposed approaches in other UAV-specific challenges, especially in low resolution and fast motion.

After stage-1 for adaptive anchor proposal generation, stage 2 will refine the proposed anchors based on the fused feature map, which fuses a deeper layer with the anchor proposal layer to raise the semantic information along with the anchor proposal knowledge. The contributions of this work are as follows:

- A novel no-prior anchor proposal network (APN) is developed to enable adaptive and lightweight anchor generation, significantly improving the adaptivity and generality of SiamAPN in the aerial scenarios.
- An elaborate feature fusion network is proposed to ensure the information flow uninterrupted, further enhancing the semantic knowledge of feature map and location awareness of tracker based on APN.
- The proposed method, siamese anchor proposal network (SiamAPN), has shown competitive performance on three challenging aerial tracking benchmarks with a high speed of ~ 200 FPS.

II. RELATED WORK

Generally, as a result of its high-speed, DCF-based trackers have been widely adopted on UAV tracking. The DCF-based approach took the object tracking algorithms to a new level, greatly promoted the robustness and accuracy with satisfying speed [5], [15]–[17]. In recent years, siamese-based trackers have become attractive due to its state-of-the-art performance which is also another choice for UAV tracking.

With the development of the convolutional neural network (CNN), the advantage of deep-learning is magnified. Meanwhile, the siamese-based network also shows its potential. After the SINT [18] transferred the tracking task into matching the patch, SiamFC [19] proposed an end-to-end method of tracking by employing a fully-convolutional neural network to learn similarity. Notwithstanding, their performance is still suboptimal. Therefore, DSiam [20] applied the target and background transformation method. Regarding visual tracking as a classification®ression task, SiamRPN introduced a region proposal network (RPN) into the siamese-based framework to improve accuracy and robustness. To overcome the influence of distractor during tracking, DaSiamRPN [13] proposes a method of utilizing the information of background. SiamRPN++ [9] applies Resnet [21] as

the backbone and achieves state-of-the-art performance by stacking the RPN module. There is no doubt that the anchor-based method improves accuracy significantly. Nevertheless, it brings hyper-parameters which decreases the tracker generality. Due to the movement of the anchors center point caused by regressing, it also brings errors to classification results. To handle those problems, anchor-free trackers are proposed, *e.g.*, SiamFC++ [10], SiamCAR [14]. They eliminated the above classification errors by fixing the center point and regressing the four offsets.

Different from the anchor-free method, we apply a novel two-stage method to handle the anchor-based problems above. Meanwhile, the proposed method utilizes adaptive anchors for achieving impressive performance. The experiments on three UAV benchmarks demonstrate that the no-prior strategy of generating anchors achieves competitive performance with high-speed.

III. PROPOSED METHOD

In this section, the proposed SiamAPN is introduced in detail. As shown in Fig. 2, SiamAPN consists of four sub-networks, respectively the feature extraction network, APN, feature fusion network, and multi-classification®ression network.

A. Feature extraction network

The feature extraction network consists of a siamese network, which has two share-architecture branches, *i.e.*, the template branch and the search branch. The inputs of these two branches are respectively a template image (denoted as z) and a search image (denoted as x). Undergoing five *conv* blocks, the outputs corresponding to the inputs are $\varphi_5(x)$ and $\varphi_5(z)$, each with 256 channels. To generate adaptive anchors, the feature maps extracted by the *conv4* block, *i.e.*, $\varphi_4(x)$ and $\varphi_4(z)$ with 384 channels, are introduced into the APN.

B. Anchor proposal network

For the sake of boosting efficiency without sacrificing the tracking performance, this work is proposed to reduce the numerous anchors and get full use of them. To this end, an anchor proposal network is constructed. As illustrated in Fig. 2 the APN utilizes the output of the penultimate *conv* layer ($\varphi_4(x)$, $\varphi_4(z)$) for anchor proposal. $\varphi_4(x)$ and $\varphi_4(z)$ are then convoluted with a 3×3 kernel. Beneficial by the convolution operator, deeper semantic information is extracted, thus leading to more comprehensive appearance learning and more robust anchors. Afterward, inspired by [9], a depth-wise cross-correlation layer is cooperated to produce similarity map as:

$$R_1 = \mathcal{F}_1(\varphi_4(x)) \star \mathcal{F}_2(\varphi_4(z)), \quad (1)$$

where \star denotes the depth-wise cross-correlation operation and $\mathcal{F}_1(\cdot)$, $\mathcal{F}_2(\cdot)$ represent different convolution operation. The response map R_1 has the same channels as $\varphi_4(x)$ which contains the information of object.

Undergoing a convolution integral calculation, the adaptive anchors are obtained. The APN produces one anchor for each

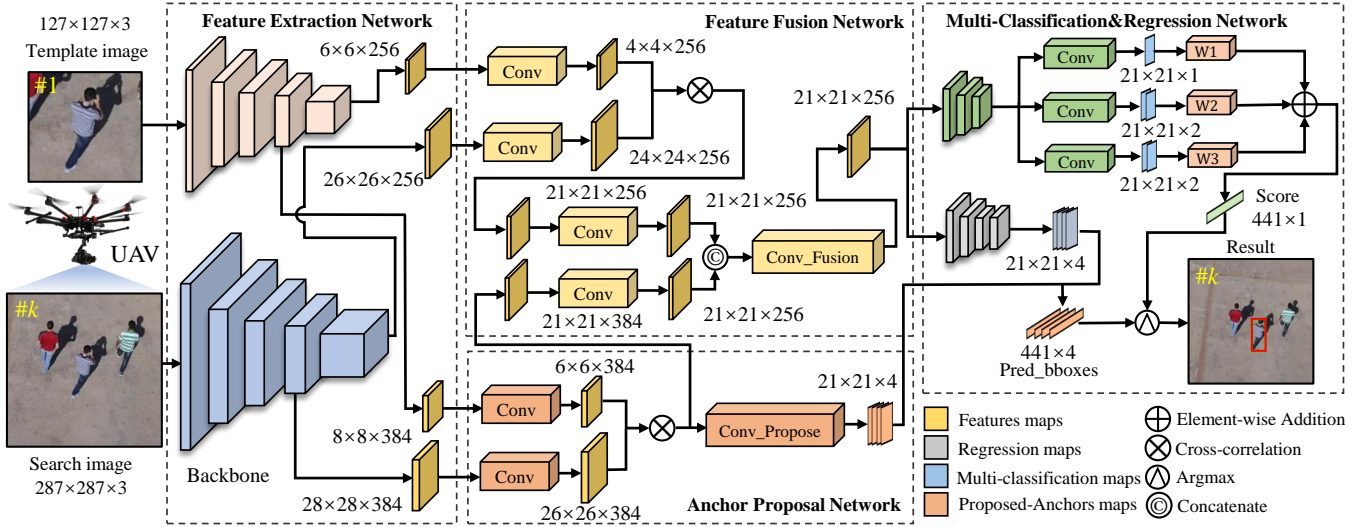


Fig. 2. The overview of SiamAPN tracker. It composes of four subnetworks, *i.e.*, feature extraction network, feature fusion network, anchor proposal network (APN), and multi-classification®ression network.

point in similarity map. For each location on the proposed anchor map $D(i, j, :)$, it can be mapped to the search patch. For instance, the position (i, j) on proposed anchor map corresponds to the location (p_i, p_j) , which is the center of the receptive field of (i, j) :

$$\begin{aligned} p_i &= \frac{w_s}{2} + \left(i - \frac{w}{2}\right) \times s, \\ p_j &= \frac{h_s}{2} + \left(j - \frac{h}{2}\right) \times s, \end{aligned} \quad (2)$$

where w_s and h_s denote the width and height of x . s presents the total stride of the network. As illustrated in Fig. 3, the proposed anchor map $D(i, j, :)$ corresponds to the distance between the point p (p_i, p_j) and proposed anchors.

Remark 1: In the anchor-based method, the anchors whose intersection over union (IoU) with ground truth are within a certain range are ignored in classification. Uniquely, since APN gives anchors adaptive characteristics, most anchors are put to good use including those ignored samples in the anchor-based method. Moreover, the experiments demonstrate its effectiveness.

Denoting (g_{x1}, g_{y1}) and (g_{x2}, g_{y2}) the left-top and right-bottom corners of the ground truth bounding box, the regression label of the proposed anchors $\tilde{x}_{(i,j)}$ can be calculated by:

$$\begin{aligned} \tilde{x}_{(i,j)}^0 &= p_i - g_{x1}, \quad \tilde{x}_{(i,j)}^1 = p_j - g_{y1}, \\ \tilde{x}_{(i,j)}^2 &= g_{x2} - p_i, \quad \tilde{x}_{(i,j)}^3 = g_{y2} - p_j. \end{aligned} \quad (3)$$

Apparently, the points far away from the center of the target tend to produce imprecise bounding boxes, which degrade the performance of the tracking system. To remove these outliers, a quality weight, *i.e.*, $\mathcal{W}(\cdot)$, is incorporated to the regression loss as:

$$\mathcal{L}_{apn} = \sum_{i,j} \mathcal{W}(p_i, p_j) L_1(D(i, j, :), \tilde{x}_{(i,j)}^n), \quad (4)$$

where L_1 is L_1 loss and $D(i, j, :)$ represents the proposed anchor map.

Although the anchor regression does not shift the center point directly, by regressing four offsets the center and size of anchors are shifty to adapt to the variable appearance of different objects.

Remark 2: Different from pre-defined anchors, the location and size of proposed anchors are flexible to adapt the variable scenes during tracking, especially in low resolution, fast motion, and occlusion. Moreover, the semantic information of adaptive anchors also contributes to accurate classification and robust regression.

C. Feature fusion network

After obtaining the proposed anchors, each point (i, j) on the response map $D(i, j, :)$ has an adaptive anchor to locate the object coarsely. Nevertheless, the approach of adaptive anchors is a double-edged sword, bring difficulties to regression. To eliminate this drawback, the feature fusion network is created to bridge the gap between APN and the classification®ression network. By applying the feature maps $(\varphi_5(x), \varphi_5(z))$ produced by feature extraction networks, the second similarity map R_2 can be calculated by:

$$R_2 = \mathcal{F}_3(\varphi_5(x)) \star \mathcal{F}_4(\varphi_5(z)). \quad (5)$$

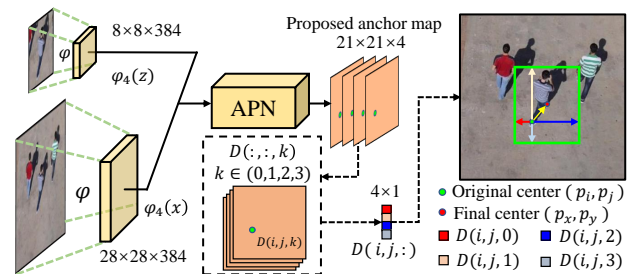


Fig. 3. Visualization of anchor proposing workflow. Each point on proposed anchor map (denoted as a green point) corresponds to a certain point on the search patch x . By calculating four offsets, the anchors can actively adapt to the appearance of different objects.

Some previous methods [14] take advantage of fusing both low-level and high-level features to improve tracking accuracy. Differently, we fuse the feature maps from APN and feature extraction network, *i.e.*, R_3 . Besides, the channel-wise concatenation is performed as:

$$R_3 = \text{Cat}(\mathcal{F}_5(R_2), \mathcal{F}_6(R_1)) , \quad (6)$$

where R_3 has 2×256 channels. To make preparation for multi-classification®ression, the response map R_3 is convoluted with 1×1 kernel to reduce its channels to 256 (denoted as R_3^*), decreasing the computational load.

Remark 3: The information of proposed anchors that provides the candidate bounding boxes for regression, together with high-level appearance features, are incorporated, enhancing the semantic knowledge of feature map and further improving the performance of SiamAPN.

D. Multi-classification®ression network

After obtaining the proposed anchor map $D(i, j, :)$, each point has a corresponding anchor. In order to further promote the performance of classifying, three classification branches are utilized. The first branch aims to determine the anchor having the largest IoU with ground truth. The second branch concentrates on selecting the points on $D(i, j, :)$ that fall in certain areas. The last branch considers the center distance between each point and ground truth center point inspired by [14].

Eventually, as illustrated in Fig. 2, the classification branch outputs three classification maps ($H_{w \times h \times 2}^{cls1}$, $H_{w \times h \times 2}^{cls2}$, and $H_{w \times h \times 1}^{cls3}$). The first branch focuses on classifying those positive anchors by calculating overlap between anchors and the ground truth bounding box. The second branch puts the center point of the proposed anchors into consideration. Besides, the distance between the final center point and ground truth is also be calculated by the third branch for accurate classifying. Integrating these three branches, the overall classification loss function is calculated as:

$$\mathcal{L}_{cls} = \lambda_{cls1} \mathcal{L}_{cls1} + \lambda_{cls2} \mathcal{L}_{cls2} + \lambda_{cls3} \mathcal{L}_{cls3} , \quad (7)$$

where \mathcal{L}_{cls1} , \mathcal{L}_{cls2} both are the cross-entropy loss functions and \mathcal{L}_{cls3} represents the *BCEWithLogitsLoss*. λ_{cls1} , λ_{cls2} , λ_{cls3} are the coefficients to weight these three branches. Each point in $H_{w \times h \times 2}^{cls1}$ contains 2D vector represents the quality evolution of each anchor. $H_{w \times h \times 2}^{cls2}$ and $H_{w \times h \times 1}^{cls3}$ concentrate on estimating the foreground and background scores of corresponding location.

The regression branch outputs a regression feature map $H_{w \times h \times 4}^{loc}$ (denoting w and h as the width and height of R_3^* respectively). $H_{w \times h \times 4}^{loc}$ uses a 4D vector ($\tilde{r}_{(i,j)}^0, \tilde{r}_{(i,j)}^1, \tilde{r}_{(i,j)}^2, \tilde{r}_{(i,j)}^3$) to represent the label of regression. Let g_x, g_y, g_w, g_h denote the center point, height and width of the ground truth boxes respectively, the distance is obtained as:

$$\begin{aligned} \tilde{r}_{(i,j)}^0 &= \frac{g_x - p_x}{p_x} , & \tilde{r}_{(i,j)}^1 &= \frac{g_y - p_y}{p_y} , \\ \tilde{r}_{(i,j)}^2 &= \ln \frac{g_w}{p_w} , & \tilde{r}_{(i,j)}^3 &= \ln \frac{g_h}{p_h} , \end{aligned} \quad (8)$$

where $p' = (p_x, p_y, p_w, p_h)$ represents center point and shape of the proposed anchor boxes which can be calculated by:

$$p' = \mathcal{G}(D(i, j, :), p) , \quad (9)$$

where \mathcal{G} represents the transformation of calculating the proposed anchor from the offset $D(i, j, :)$ and original center p . Putting the advantage of different loss functions into consideration, we adopt a *smooth L1loss* and *IoUloss* for regression. Consequently, the regression loss is computed as:

$$\begin{aligned} \mathcal{L}_{loc} &= \lambda_{loc1} L_{IOU}(\mathcal{T}(H^{loc}(i, j, :), p'), g) + \\ &\lambda_{loc2} L1(H^{loc}(i, j, :), \tilde{r}_{(i,j)}) , \end{aligned} \quad (10)$$

where $g = (g_{x1}, g_{y1}, g_{x2}, g_{y2})$ is ground truth bounding box and \mathcal{T} aims to transfer the $H^{loc}(i, j, :)$ to predicted boxes for calculating *IoUloss*.

Put all loss functions together, the overall loss function is as follows:

$$\mathcal{L} = \mathcal{L}_{apn} + \lambda_1 \mathcal{L}_{cls} + \lambda_2 \mathcal{L}_{loc} , \quad (11)$$

where λ_1, λ_2 are the coefficients to weight the classification loss and regression loss.

IV. EXPERIMENT

In this section, the proposed method is comprehensively evaluated on three well-known authoritative UAV tracking benchmarks, *i.e.*, VisDrone2018-SOT-test [22], UAV20L [11], and UAV123@10fps [11]. 10 deep-learning based trackers are involved in the evaluation. Classifying by tracking speed, they can be divided as real-time trackers, *i.e.*, SiamRPN++ [9], DaSiamRPN [13], SiamFC++ [10], SiamFC [19], UDT [23], UDT+ [23], TADT [24], DSiam [25], CoKCF [26], and non-real-time tracker, *i.e.*, CF2 [27].

Remark 4: For the sake of fairness, all trackers are equipped with the same backbone, *i.e.*, AlexNet [28] which is pre-trained on ImageNet [29]. Note that, all parameters of those trackers are consistent with their paper respectively.

A. Implementation details

SiamAPN uses the AlexNet as the backbone with the parameters of the first two convolution layers frozen and only fine-tune the last three convolution blocks. There are a total of 50 epochs. For the first 10 epochs, the parameters of the feature extraction network are frozen to train the APN, feature fusion network, and multi-classification®ression network. For the last 40 epoch, the whole network is end-to-end trained with learning rate decayed from 0.005 to 0.0005 in log space. Meanwhile, our network is trained with SGD with a minibatch of 124 pairs. The momentum of 0.9 is used. During the process of training, except λ_{cls1} is set to 1.2, other parameters, *i.e.*, λ_{cls2} , λ_{cls3} , λ_{loc1} , and λ_{loc2} , are set to 1. As for the input size of the template patch and search patch, they are set to 127×127 pixels and 287×287 pixels, respectively. The tracking code is available at <https://github.com/vision4robotics/SiamAPN>.

Images from COCO [30], ImageNet VID [31], GOT-10K [32] and Youtube-BB [33] are extracted to train our

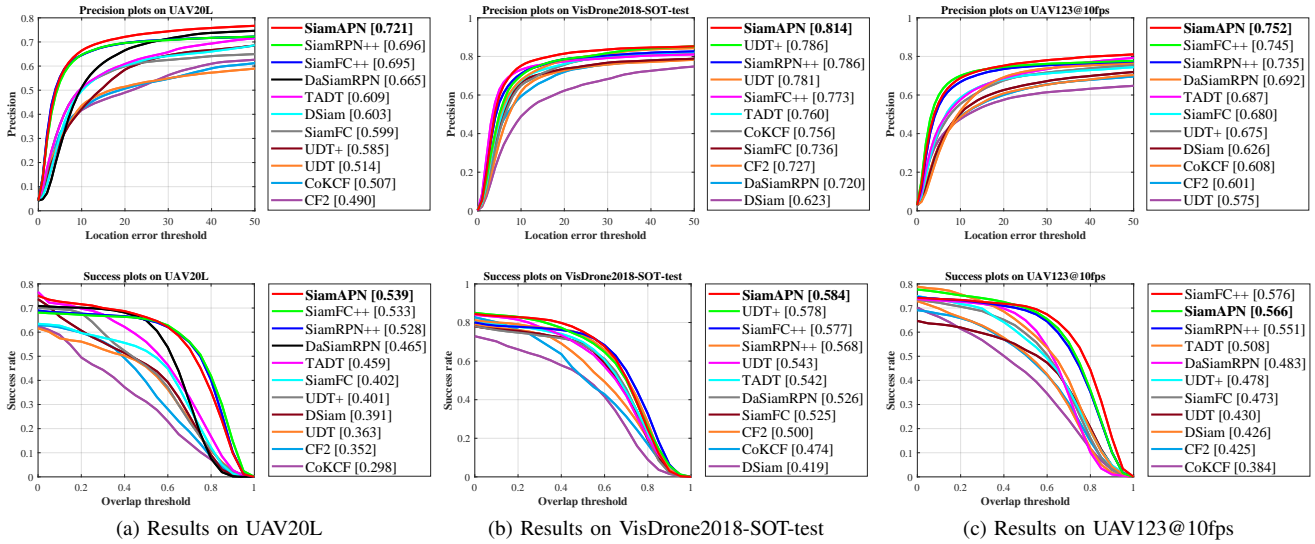


Fig. 4. Overall performance of all trackers on (a) UAV20L, (b) VisDrone2018-SOT-test, and (c) UAV123@10fps. The experimental results demonstrate that our method yields superior performance on all benchmarks.

tracker. The proposed method is implemented in Python using Pytorch on a PC with an Intel i9-9920X CPU, a 32GB RAM, and an Nvidia TITAN RTX GPU.

B. Evaluation metrics

The experiments are based on one-pass evaluation (OPE) [34], *i.e.*, precision and success rate. The success rate is measured as IoU. The success plot represents the percentage of the frames whose IoU is larger than a preset threshold. The area-under-the-curve (AUC) on the success plot is utilized for ranking. Besides, the precision is measured by the center location error (CLE) between the estimated bounding box and the ground truth bounding box. The precision plot shows the percentage of scenarios whose distance between the estimated bounding box and ground truth one is smaller than different thresholds and the score at 20 pixels is used for ranking.

C. Evaluation on UAV benchmarks

1) *Overall performance:* The proposed method outperforms other state-of-the-art trackers competitively on all three benchmarks.

UAV20L: Consisting of 20 long-term sequences (2934 frames per sequence on average) with various challenging scenes including over 58k frames, UAV20L [11] is designed especially for practical tracking. As shown in Fig. 4, SiamAPN performs favorably with an improvement of 2.5% on precision and 0.6% on AUC score comparing to the second-best tracker.

TABLE I

AVERAGE PRECISION AS WELL AS AUC SCORE OF TOP 5 TRACKERS ON THREE BENCHMARKS. **RED** AND **GREEN** FONTS INDICATE THE FIRST AND SECOND BEST RESULTS RESPECTIVELY.

Trackers	SiamAPN	SiamFC++	SiamRPN++	DaSiamRPN	TADT
Precision (%)	76.2	73.7	73.9	69.2	68.5
AUC (%)	56.3	56.2	54.9	49.1	50.3

VisDrone2018-SOT-test: For evaluating the tracking algorithms in complex conditions, the VisDrone2018-SOT-test [22] is created for UAV tracking with numerous visual challenges. As shown in Fig. 4, SiamAPN has outperformed all other trackers in terms of precision (0.814) and AUC (0.584), followed by UDT+ (0.786, 0.578).

UAV123@10fps: Consisting of 123 sequences, UAV123@10fps [11] is downsampled from a 30FPS version of sequences. Since the frame interval becomes larger, the challenges of many scenarios are increased, such as fast motion and low resolution. Consequently, to evaluate the ability of trackers in the face of fast motion comprehensively, UAV123@10fps [11] is more appropriate than UAV123. The tracking performances of all trackers are presented in Fig. 4, SiamAPN ranks first in terms of precision (0.752), while maintaining favorable result on success rate (0.566).

The continuous competitive performance on the three benchmarks demonstrates the robustness of SiamAPN. To validate the top rank trackers in more detail, TABLE I presents the average precision and AUC of the top 5 trackers in three benchmarks, respectively. SiamAPN achieves the best performance in terms of precision and AUC score. Especially, SiamAPN has achieved an average improvement of 2.3% in precision (0.762) compared to SiamRPN++ (0.739). Some qualitative evaluations are demonstrated in Fig. 6.

2) *Attribute-based performance:* Attribute-based evaluation results on UAV benchmarks are shown in Fig. 5. We compare the AUC score of the UAV-specific attributes of the top 5 trackers. Attributing to the flexible anchors generated by APN, SiamAPN can avoid neglecting objects in different scenes. In the fast motion scenarios, SiamAPN improves SiamFC++ by 3.9% in the AUC score on average and improves SiamRPN++ by 5.1% in the AUC score on average. In partial occlusion, full occlusion, and low resolution, SiamAPN has a superiority of 1.1%, 4%, and 3.9% (AUC) on average respectively compared to SiamFC++ by utilizing

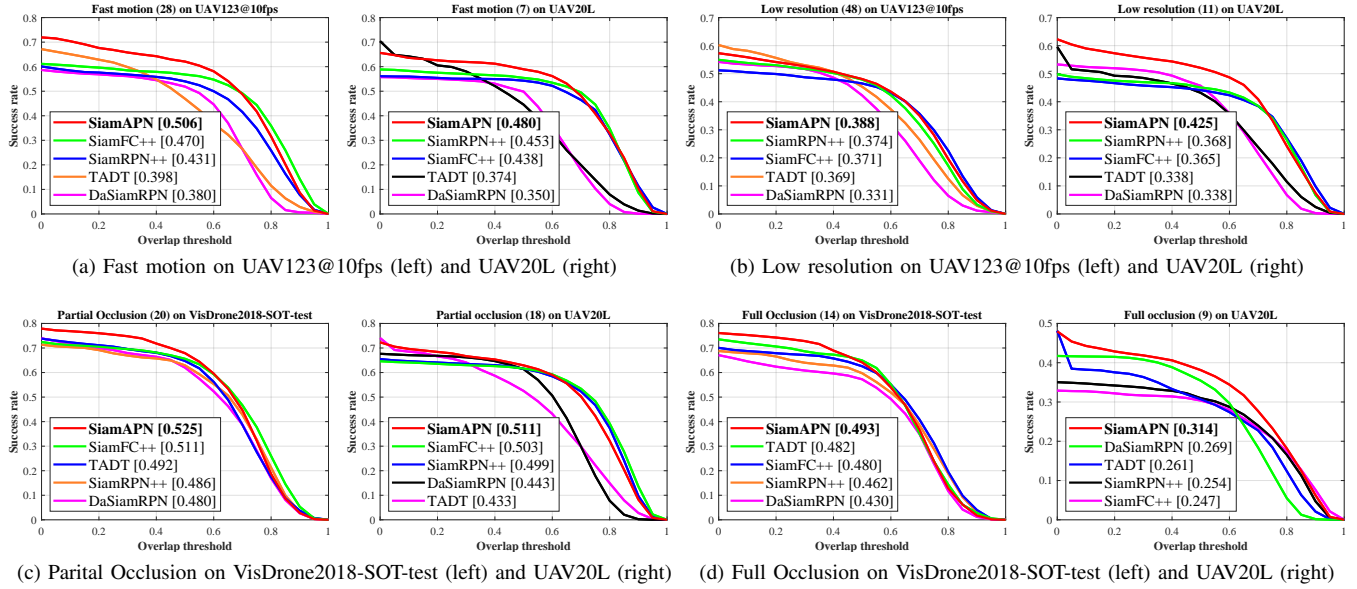


Fig. 5. Attribute-based comparison with top 5 trackers on four UAV-specific challenges, *i.e.*, fast motion, low resolution, partial, and full occlusion. It shows that SiamAPN maintains robustness in different conditions.

flexible anchors. In addition, SiamAPN also outperforms significantly SiamRPN++ in terms of partial occlusion by 2.55%, full occlusion by 4.55%, and low resolution by 3.55% on average. These cheerful results demonstrate the robustness of SiamAPN in various UAV tracking conditions.

3) *Key parameter analysis*: To analyze the influence of the classification weight λ_{cls1} , λ_{cls1} is set to different values for analyzing. Starting from 0.58, λ_{cls1} increases in a small step of 0.1 until 1.78. When approaching the best point, the step size is further reduced to 0.02. As shown in Fig. 7, as λ_{cls1} increases, more attention is paid to the classification of adaptive anchors, the AUC and precision of SiamAPN improve gradually, demonstrating the effectiveness of the APN. When λ_{cls1} is set to 1.18, the AUC and precision reach the highest point. However, as λ_{cls1} continues to increase, too much attention is drawn to the APN classification branch, the information in the other two branches are not assigned

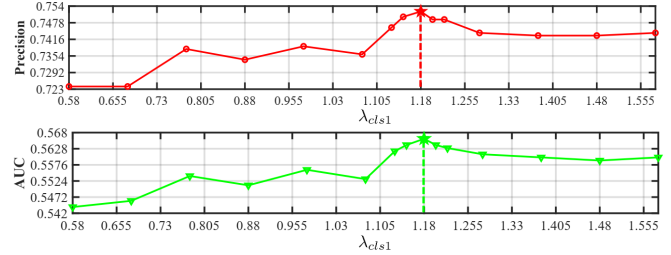


Fig. 7. Key parameter analysis of λ_{cls1} on UAV123@10fps. When the $\lambda_{cls1} = 1.18$, SiamAPN achieves the best overall performance.

enough weight to the performance. Therefore, when λ_{cls1} is set to an appropriate value, APN can indeed favorably boost the tracking performance. Consequently, $\lambda_{cls1} = 1.18$ is chosen for the best performance.

V. CONCLUSION

In this work, for the sake of balancing efficiency and robustness, a novel two-stage high-speed tracking approach is proposed. The design of adaptive anchors makes SiamAPN sensitive and robust to different objects under various scenes especially in fast motion, occlusion, and low resolution. Meantime, APN avoids hyper-parameters associated with the anchors and decreases numerous anchors, making our tracker general and efficient to different scenes. Besides, by fusing the feature maps, the information flow is protected, further enhancing the semantic knowledge of feature maps and location consciousness of SiamAPN. The experiments on multiple UAV benchmarks corroborate the competitive performance of SiamAPN. Consequently, we are convinced that our work can promote the development of UAV tracking related applications.

ACKNOWLEDGMENT

This work is supported by the National Natural Science Foundation of China (No. 61806148) and the Natural Science Foundation of Shanghai (No. 20ZR1460100).

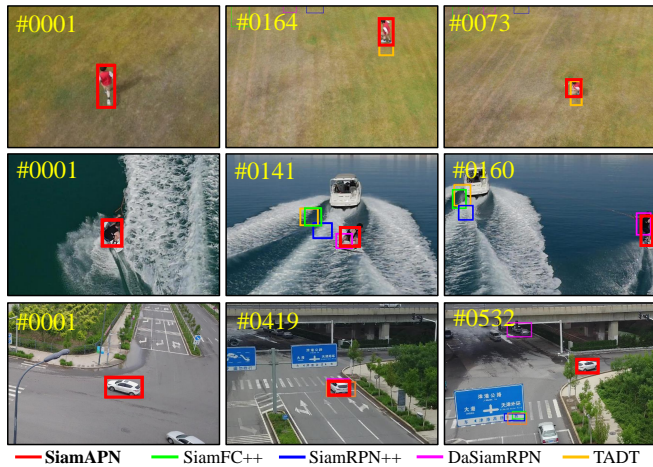


Fig. 6. Screenshots of *bike3*, *wakeboard4* from UAV123@10fps, and *uav0000180_00050_s* from VisDrone2018-SOT-test. More tracking videos can be found here: <https://youtu.be/tp3YtB2XHVK>.

REFERENCES

- [1] M. Odelga, P. Stegagno, N. Kochanek, and H. H. Bühlhoff, "A Self-contained Teleoperated Quadrotor: On-Board State-Estimation and Indoor Obstacle Avoidance," in *Proceedings of the IEEE International Conference on Robotics and Automation (ICRA)*, 2018, pp. 7840–7847.
- [2] C. Yuan, Z. Liu, and Y. Zhang, "Aerial images-based forest fire detection for firefighting using optical remote sensing techniques and unmanned aerial vehicles," *Journal of Intelligent & Robotic Systems*, vol. 88, no. 2-4, pp. 635–654, 2017.
- [3] D. R. McArthur, A. B. Chowdhury, and D. J. Cappelleri, "Autonomous Control of the Interacting-BoomCopter UAV for Remote Sensor Mounting," in *Proceedings of the IEEE International Conference on Robotics and Automation (ICRA)*, 2018, pp. 5219–5224.
- [4] Z. Huang, C. Fu, Y. Li, F. Lin, and P. Lu, "Learning Aberrance Repressed Correlation Filters for Real-time UAV Tracking," in *Proceedings of the IEEE International Conference on Computer Vision (ICCV)*, 2019, pp. 2891–2900.
- [5] Y. Li, C. Fu, F. Ding, Z. Huang, and G. Lu, "AutoTrack: Towards High-Performance Visual Tracking for UAV With Automatic Spatio-Temporal Regularization," in *Proceedings of the IEEE/CVF Conference on Computer Vision and Pattern Recognition (CVPR)*, 2020, pp. 11 920–11 929.
- [6] F. Li, C. Fu, F. Lin, Y. Li, and P. Lu, "Training-Set Distillation for Real-Time UAV Object Tracking," in *Proceedings of the IEEE International Conference on Robotics and Automation (ICRA)*, 2020, pp. 9715–9721.
- [7] Y. Li, C. Fu, Z. Huang, Y. Zhang, and J. Pan, "Keyfilter-Aware Real-Time UAV Object Tracking," in *Proceedings of the IEEE International Conference on Robotics and Automation (ICRA)*, 2020, pp. 193–199.
- [8] C. Fu, Z. Huang, Y. Li, R. Duan, and P. Lu, "Boundary Effect-Aware Visual Tracking for UAV with Online Enhanced Background Learning and Multi-Frame Consensus Verification," in *Proceedings of the IEEE/RSJ International Conference on Intelligent Robots and Systems (IROS)*, 2019, pp. 4415–4422.
- [9] B. Li, W. Wu, Q. Wang, F. Zhang, J. Xing, and J. Yan, "SiamRPN++: Evolution of Siamese Visual Tracking With Very Deep Networks," in *Proceedings of the IEEE/CVF Conference on Computer Vision and Pattern Recognition (CVPR)*, 2019, pp. 4277–4286.
- [10] Y. Xu, Z. Wang, Z. Li, Y. Yuan, and G. Yu, "SiamFC++: Towards Robust and Accurate Visual Tracking with Target Estimation Guidelines," in *Proceedings of the AAAI Conference on Artificial Intelligence (AAAI)*, 2020, pp. 12 549–12 556.
- [11] M. Mueller, N. Smith, and B. Ghanem, "A Benchmark and Simulator for UAV Tracking," in *Proceedings of the European Conference on Computer Vision (ECCV)*, 2016, pp. 445–461.
- [12] B. Li, J. Yan, W. Wu, Z. Zhu, and X. Hu, "High Performance Visual Tracking with Siamese Region Proposal Network," in *Proceedings of the IEEE/CVF Conference on Computer Vision and Pattern Recognition (CVPR)*, 2018, pp. 8971–8980.
- [13] Z. Zhu, Q. Wang, B. Li, W. Wu, J. Yan, and W. Hu, "Distractor-aware siamese networks for visual object tracking," in *Proceedings of the European Conference on Computer Vision (ECCV)*, 2018, pp. 101–117.
- [14] D. Guo, J. Wang, Y. Cui, Z. Wang, and S. Chen, "SiamCAR: Siamese Fully Convolutional Classification and Regression for Visual Tracking," in *Proceedings of the IEEE/CVF Conference on Computer Vision and Pattern Recognition (CVPR)*, 2020, pp. 6268–6276.
- [15] J. F. Henriques, R. Caseiro, P. Martins, and J. Batista, "High-speed tracking with kernelized correlation filters," *IEEE Transactions on Pattern Analysis and Machine Intelligence*, vol. 37, no. 3, pp. 583–596, 2014.
- [16] H. K. Galoogahi, A. Fagg, and S. Lucey, "Learning Background-Aware Correlation Filters for Visual Tracking," in *Proceedings of the IEEE International Conference on Computer Vision (ICCV)*, 2017, pp. 1144–1152.
- [17] C. Fu, J. Ye, J. Xu, Y. He, and F. Lin, "Disruptor-Aware Interval-Based Response Inconsistency for Correlation Filters in Real-Time Aerial Tracking," *IEEE Transactions on Geoscience and Remote Sensing*, pp. 1–13, 2020.
- [18] R. Tao, E. Gavves, and A. W. M. Smeulders, "Siamese Instance Search for Tracking," in *Proceedings of the IEEE/CVF Conference on Computer Vision and Pattern Recognition (CVPR)*, 2016, pp. 1420–1429.
- [19] L. Bertinetto, J. Valmadre, J. F. Henriques, A. Vedaldi, and P. H. Torr, "Fully-convolutional siamese networks for object tracking," in *Proceedings of the European Conference on Computer Vision (ECCV)*, 2016, pp. 850–865.
- [20] Q. Guo, W. Feng, C. Zhou, R. Huang, L. Wan, and S. Wang, "Learning Dynamic Siamese Network for Visual Object Tracking," in *Proceedings of the IEEE International Conference on Computer Vision (ICCV)*, 2017, pp. 1781–1789.
- [21] K. He, X. Zhang, S. Ren, and J. Sun, "Deep Residual Learning for Image Recognition," in *Proceedings of the IEEE/CVF Conference on Computer Vision and Pattern Recognition (CVPR)*, 2016, pp. 770–778.
- [22] L. Wen, P. Zhu, D. Du, X. Bian, H. Ling, Q. Hu, C. Liu, H. Cheng, X. Liu, W. Ma, *et al.*, "Visdrone-sot2018: The vision meets drone single-object tracking challenge results," in *Proceedings of the European Conference on Computer Vision (ECCV)*, 2018, pp. 1–27.
- [23] N. Wang, Y. Song, C. Ma, W. Zhou, W. Liu, and H. Li, "Unsupervised Deep Tracking," in *Proceedings of the IEEE/CVF Conference on Computer Vision and Pattern Recognition (CVPR)*, 2019, pp. 1308–1317.
- [24] X. Li, C. Ma, B. Wu, Z. He, and M. Yang, "Target-Aware Deep Tracking," in *Proceedings of the IEEE/CVF Conference on Computer Vision and Pattern Recognition (CVPR)*, 2019, pp. 1369–1378.
- [25] Q. Guo, W. Feng, C. Zhou, R. Huang, L. Wan, and S. Wang, "Learning Dynamic Siamese Network for Visual Object Tracking," in *Proceedings of the IEEE International Conference on Computer Vision (ICCV)*, 2017, pp. 1781–1789.
- [26] L. Zhang and P. N. Suganthan, "Robust visual tracking via co-trained kernelized correlation filters," *Pattern Recognition*, vol. 69, pp. 82–93, 2017.
- [27] C. Ma, J. Huang, X. Yang, and M. Yang, "Hierarchical Convolutional Features for Visual Tracking," in *Proceedings of the IEEE International Conference on Computer Vision (ICCV)*, 2015, pp. 3074–3082.
- [28] A. Krizhevsky, I. Sutskever, and G. E. Hinton, "Imagenet classification with deep convolutional neural networks," in *Advances in neural information processing systems (NIPS)*, 2012, pp. 1097–1105.
- [29] O. Russakovsky, J. Deng, H. Su, J. Krause, S. Satheesh, S. Ma, Z. Huang, A. Karpathy, A. Khosla, M. Bernstein, A. Berg, and L. Fei-Fei, "ImageNet Large Scale Visual Recognition Challenge," *International Journal of Computer Vision*, vol. 115, 09 2014.
- [30] T.-Y. Lin, M. Maire, S. Belongie, J. Hays, P. Perona, D. Ramanan, P. Dollár, and C. L. Zitnick, "Microsoft coco: Common objects in context," in *Proceedings of the European conference on computer vision (ECCV)*, 2014, pp. 740–755.
- [31] O. Russakovsky, J. Deng, H. Su, J. Krause, S. Satheesh, S. Ma, Z. Huang, A. Karpathy, A. Khosla, M. Bernstein, *et al.*, "Imagenet Large Scale Visual Recognition Challenge," *International Journal of Computer Vision*, vol. 115, no. 3, pp. 211–252, 2015.
- [32] L. Huang, X. Zhao, and K. Huang, "GOT-10k: A Large High-Diversity Benchmark for Generic Object Tracking in the Wild," *IEEE Transactions on Pattern Analysis and Machine Intelligence*, pp. 1–1, 2019.
- [33] E. Real, J. Shlens, S. Mazzocchi, X. Pan, and V. Vanhoucke, "YouTube-BoundingBoxes: A Large High-Precision Human-Annotated Data Set for Object Detection in Video," in *Proceedings of the IEEE/CVF Conference on Computer Vision and Pattern Recognition (CVPR)*, 2017, pp. 7464–7473.
- [34] Y. Wu, J. Lim, and M. Yang, "Online object tracking: A benchmark," in *Proceedings of the IEEE Conference on Computer Vision and Pattern Recognition*, 2013, pp. 2411–2418.